JOURNAL OF PROPULSION AND POWER
Vol. 10, No. 5, Sept.–Oct. 1994

Characterization of Abrupt Rotating Stall Initiation in an Axial Flow Compressor

Patrick B. Lawless,* Kuk H. Kim,† and Sanford Fleeter‡
Purdue University, West Lafayette, Indiana 47907

The detection of rotating stall precursors has become a focus of current research because of the desirability of implementing a control scheme well before a compressor enters a stall condition. To identify spatially coherent pressure waves that would serve as precursors to the development of an instability in a low-speed, axial-flow compressor, the Purdue Axial Flow Research Compressor was instrumented with sensitive electret microphones uniformly distributed around the compressor circumference. Fourier analysis of simultaneously sampled data from these microphone arrays was employed to identify the development of dominant spatial modes in the pressure field in the compressor. The transition to stall was observed to be an abrupt process, with the eruption of a stall cell on rotor blades corresponding to a strong rise in the spatial mode magnitude. However, a weak, circumferentially distorted pressure wave was detected that began adjusting to the ultimate phase propagation velocity of the finite stall pattern from within 5–26 revolutions prior to a significant rise in the mode magnitude and the indication of a stall cell on the rotor blade. Comparison of the first and second harmonics of this signal indicate that this disturbance is represented in the spatial domain by an impulsive-type waveform, and thus likely represents a small, propagating flow separation.

Nomenclature

f_t = frequency measured by a single transducer
N = number of transducers in spatial array
n = mode number
t = time
V_p = phase angular velocity
α = mode phase angle

Introduction

THE surge line represents a demarcation between stable compressor operating points and those wherein unsteady flow phenomena dominate. However, the term "surge line" is somewhat misleading since two types of unsteady flow phenomena are possible: 1) rotating stall or 2) surge. Rotating stall and surge are flow instabilities that seriously limit the performance of turbomachines as well as their durability. Surge refers to a global oscillation of the mass flow through the compression system. Surge is regarded as a phenomena of the entire compression system, consisting of the compressor and the system into which it discharges. Rotating stall, in contrast, is an instability local to the compressor itself, and is characterized by a circumferentially nonuniform mass deficit that propagates around the compressor annulus at a fraction of wheel speed. Rotating stall often manifests itself in a compressor that is simultaneously experiencing surge. Current generation turbomachines must allow for a safety margin that places the operating point in a region far enough removed from the surge line to prevent the onset of these instabilities.

Presented as Paper 93-2238 at the AIAA/SAE/ASME/ASEE 29th Joint Propulsion Conference and Exhibit, Monterey, CA, June 28–30, 1993; received July 19, 1993; revision received Feb. 4, 1994; accepted for publication Feb. 5, 1994. Copyright © 1993 by the authors. Published by the American Institute of Aeronautics and Astronautics, Inc., with permission.

*Assistant Professor, School of Mechanical Engineering. Member AIAA.
†AFRAPT Trainee, School of Mechanical Engineering. Member AIAA.
‡Professor, School of Mechanical Engineering. Associate Fellow AIAA.

Attempts to increase the stable operating range of compressors have recently encompassed the concept of active control. Definitive success has been achieved in the suppression of surge in centrifugal compressors, as reported by researchers such as Pinsley et al.[1] and Ffowcs Williams and Graham.[2] Equally promising results have been demonstrated for rotating stall in low-speed axial compressors by both Day[3] and Paduano.[4]

Because of the desirability of implementing a control scheme well before the compressor enters a finite surge or stall condition, the identification of precursors to these instabilities has become a focus of research. In the case of rotating stall in an axial compressor, researchers such as Garnier et al.[5] have observed that, in its early stages, rotating stall is characterized as a weak, linear disturbance that grows into a finite disturbance in a region of preferential amplification on the performance map. This concept of a "prestall" or "modal" wave type of stall initiation is in contrast to a different, and perhaps more traditional view, in which rotating stall is the result of the propagation of a finite separation zone on a rotor airfoil due to blockage effects, as described by Emmons.[6] The appearance of a finite stall cell, rather than the growth of a weak sinusoidal wave, is reported to be a primary mechanism of stall initiation in axial compressor investigations carried out by Day.[7]

The research presented here is directed at the identification of spatially coherent pressure waves that would serve as precursors to instability development, including both the initiation of rotating stall and rotating stall during a surge cycle, thereby extending the information on stall initiation in axial flow compressors. In particular, a view of stall initiation in a low-speed, three-stage axial compressor is made by utilizing Fourier analysis in the circumferential spatial domain. To this end, arrays of pressure transducers are circumferentially distributed in the o.d. endwall of the Purdue Axial Flow Research Compressor (PAFRC). The microphone arrays are sampled while bringing the compressor into an instability condition by slowly closing a throttle plate after the compressor has been allowed to reach a steady operating condition. Data acquisition is terminated when the trigger level from a single microphone reaches a previously determined level and the proper number of post-trigger samples have been acquired.

Table 1 Airfoil and compressor characteristics

Airfoil type	IGV	Rotor	Stator
Number of airfoils	36	43	31
Chord C, mm	30	30	30
Solidity	0.96	1.14	1.09
Camber Q, deg	36.9	28.0	27.7
Stagger angle g, deg	21.0	36.0	−36.0
Aspect ratio	2.0	2.0	2.0
Thickness/chord, %	10	10	10
Design flow rate, kg/s	—	2.03	—
Design axial velocity, m/s	—	24.38	—
Design rotational speed, rpm	—	2250	—
Number of stages			
Design stage pressure ratio	—	3	—
Inlet tip diameter, mm	—	1.0	—
Hub/tip radius ratio	—	420	—
Stage efficiency, %	—	0.714	—
	—	85	—

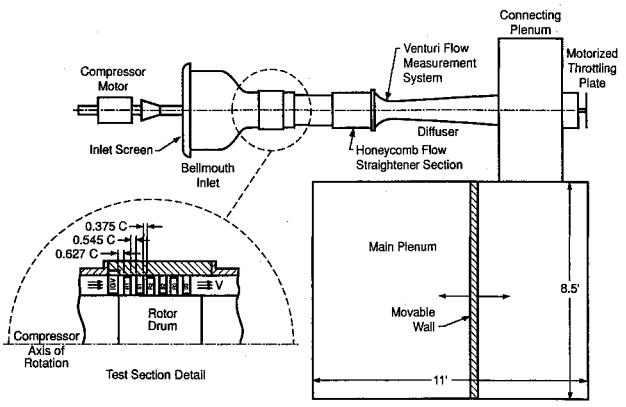

Fig. 1 Purdue axial flow research compressor.

Research Compressor

The PAFRC facility consists of a bellmouth inlet, the test section, a honeycomb flow straightener section, a venturi flow meter, a plenum, and a throttle plate. The axial velocity through this three-stage, low-speed compressor (Fig. 1) is approximately 24.4 m/s (80.1 ft/s). Each compressor stage contains 43 rotor blades and 31 stator vanes having a British C4 airfoil profile, with the first stage rotor inlet flowfield established by an inlet guide vane (IGV) row of 36 airfoils. The compressor is driven by a 15-hp variable speed dc electric motor. The overall compressor and airfoil characteristics are defined in Table 1.

The compressor plenum consists of two sections, a small connecting plenum that is directly attached in line of flow, and the main plenum. The small plenum is divided in half so that the compressor exit flow enters the bottom half of the small plenum, then enters the large plenum and flows to the throttle exit. Inside the main plenum a movable wall is used to generate different compressor volumes, and thus compressor instability modes (e.g., rotating stall or surge). The throttle plate is motorized with a variable speed control.

Instrumentation

Endwall Static Pressures

The instrumentation utilized to detect precursors to the stall condition was required to detect weak, low-frequency, spatially coherent waves in the compressor. To this end, researchers such as McDougall et al.,[8] Day,[7] and Garnier et al.[5] have employed spatial Fourier analysis of the signals from circumferentially distributed hot-wire probes with success. However, the high cost, fragility, and intrusive nature of hot-wire probes provides motivation for the use of alternate transducers for this type of analysis. A recent study of the stall

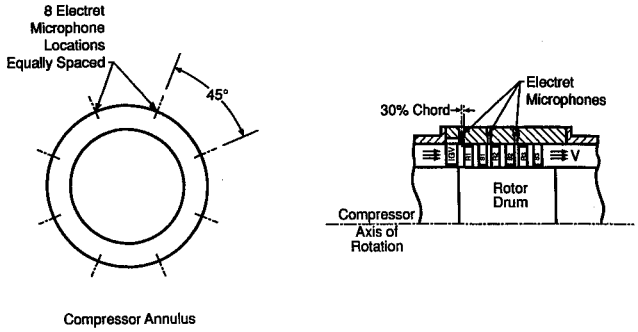

Fig. 2 Endwall static pressure electret microphone instrumentation.

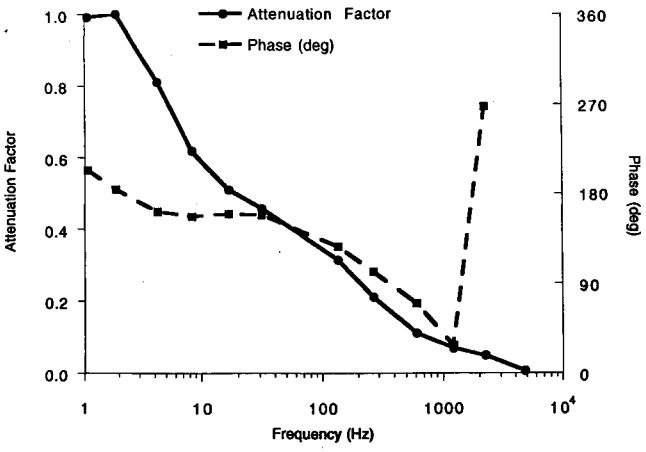

Fig. 3 Dynamic response of an electret microphone.

initiation process in a low-speed centrifugal compressor by the authors[9] successfully utilized Fourier analysis of the signals from spatial arrays of conventional audio electret microphone elements mounted in the compressor endwall to detect weak pressure disturbances. Because of their high sensitivity, these devices are ideal for detection of events at the initial stages of the compressor instability. Although the microphones show some nonlinearity in the frequency domain, they exhibit excellent amplitude linearity over a limited frequency band and also demonstrate excellent low frequency response. Based on this previous research, similar devices were chosen to characterize the initial stages of rotating stall in the PAFRC facility. Eight microphones were equally spaced around the circumference 30% chord length upstream of the first rotor stage. Two additional arrays of eight microphones each were also located 30% chord lengths upstream of the second and third rotor stages. Both the circumferential and axial locations of these microphones on the compressor are given in Fig. 2.

To prevent the high-frequency signals from rotor blade passage and flow noise from dominating the low-frequency signals of interest, a short attenuator tube is installed between the microphones and the static taps in the compressor endwall. The attenuator, consisting of a stainless steel tube of 4.5-mm diam filled with porous felt core of 5 mm length, serves as a pneumatic low-pass filter. Each microphone with its specific attenuator tube is dynamically calibrated against an Entran EPIL-6B-2 dynamic pressure transducer. Typical results from this calibration are given in Fig. 3, which presents the microphone gain magnitude relative to its maximum value. Signals at blade pass frequency are attenuated by a factor of 9 with respect to a signal at the frequency typical of rotating stall in this compressor, while a frequency of 5000 Hz marks the beginning of the stop band of the filter. With the addition of the attenuator tubes, a highly nonlinear phase response is encountered, also shown in Fig. 3. Note that the unaltered microphones produce a negative voltage for an increasing pressure that manifests itself as a response that is 180-deg out of phase with the pressure signal. Although the nonlinearity

of the frequency response precludes direct conversion of the microphone voltage output to pressure, the approach taken in processing the signals, as discussed below, minimizes this difficulty. In addition, the device linearity is not a critical requirement for this application since the overall goal of the microphone arrays is to serve as spatial wave detectors rather than fine resolution pressure transducers. To obtain the best possible results from the spatial Fourier analysis, the microphones were selected from a larger lot of 60 microphones for similar phase and magnitude response.

Velocity and Rotor Blade Pressure Measurements

The compressor first-stage rotor row is instrumented with cross hot-wire probes and rotor blade dynamic pressure transducers. Two cross-wire probes are located on the rotor drum 18.8% chord upstream and 65% blade spacing from a rotor blade. The measurement of the first-stage rotor blade midspan surface unsteady pressures is accomplished with 12 ultraminiature, high-response transducers embedded in the rotor blades. The suction surface unsteady pressures are measured at the following chordwise locations: 5, 22.3, 46, 72, and 81.3%. The pressure surface chordwise locations are 6, 22.7, 30, 47, 72, 80.7%.

Experimental Technique

Data Acquisition

Acquisition and digitization of the microphone signals is accomplished using four National Instruments NB-A2000 analog-to-digital conversion boards installed in an Apple Macintosh IIfx computer. This system allows 16 channels of simultaneously acquired data to be recorded. Data acquisition is initiated by an analog trigger signal supplied by one of the microphones upstream of the first rotor row. The boards are operated in a pretrigger mode, with samples before the trigger occurred recorded along with post-trigger data.

To bring the compressor into an instability condition, the throttle plate is slowly closed from the fully open position after the compressor has been allowed to reach a steady operating condition. Data acquisition is terminated when the trigger level from the microphone reaches a previously determined level and the proper number of post-trigger samples have been acquired. Continuous motion of the throttle plate is employed throughout the acquisition sequence. Data are acquired at a sampling frequency of 5000 Hz. Typically, 5.5 s of data is recorded, with 50% of the retained samples taken before the trigger occurred.

Spatial Domain Signal Analysis

As mentioned previously, the Fourier analysis of signals from an array of circumferentially distributed sensors has proven effective in the detection of the early stages of spatially coherent events such as rotating stall.

In a spatial domain analysis of the stall pattern, a number of circumferentially distributed transducers are sampled simultaneously. Fourier decomposition of the signal results in the representation of the signal in the modal domain. The spatial wave number or mode n reflects the number of periods of the sinusoid occurring in one circumference. As in a frequency domain transform, the relative magnitudes of the fundamental and higher modes provides an indication of the nature of the waveform. A dominant fundamental mode indicates a wave that is sinusoidally distributed around the circumference. As the higher modes grow in magnitude, the wave takes on a more impulsive distribution.

For a given sensor array, the reference point for the mode phase angle α is arbitrarily referenced to a single sensor that is chosen as the origin for the circumferential coordinate system. The rate of propagation of the stall pattern around the annulus is given by time rate of change of α, here defined as the phase angular velocity V_p:

$$V_p = \frac{d\alpha}{dt} \tag{1}$$

Although the customary units for an angular velocity are expressed as radians per unit time (e.g., rad/s), the relationship between the phase angular velocity of a modal pattern and the frequency of the stall phenomena make a phase velocity reported in hertz the most useful quantity for this investigation. Specifically

$$|V_p| = (f_t/n) \tag{2}$$

where f_t is the frequency of the stall phenomena that would be recorded by a single sensor at a fixed circumferential position. As used in this application, the phase angular velocity in hertz is a signed quantity, with the sign specifying the direction of propagation around the compressor annulus. By convention, the positive direction is taken with rotor rotation.

Data Analysis

Data from the microphones are numerically bandpass filtered using Butterworth filtering algorithms. This procedure limits noise and reduces the effects of spatial aliasing, discussed below. After filtering, each microphone signal is scaled by the appropriate gain value and then processed with the spatial Fourier transform. A finite difference estimate of the first derivative is used to calculate the phase propagation velocity of the spatial pattern V_p from the phase angle of the Fourier coefficients.

Because of the limited number of transducers that could be practically employed in the microphone arrays, the prospect of signal aliasing was of concern. Aliasing of a digitally acquired signal occurs when the sampling frequency is insufficient to allow reconstruction of the analog signal from the discrete digital data.

In a spatial domain sampling of a waveform, the number of transducers employed defines the sampling period and, hence, the effective "sampling frequency." Waves of harmonic number greater than the Nyquist (the number of transducers divided by two) will be aliased into a different harmonic, possibly creating confusion as to the actual mode shape. The numerical filtering of the microphone signals before performing the spatial Fourier analysis allowed the signals to be restricted to a bandwidth that contained only the mode shape of interest, reducing the effects of spatial aliasing.

Results and Discussion

Stall Cell Development

The results to be presented here describe the behavior of the PAFRC under conditions of rotating stall and surge. The details of the fully developed stall condition of this compressor are reported by Kim and Fleeter.[10] When the compressor is operated with a small exit plenum volume, the compressor enters a rotating stall condition as the mass through-flow is reduced. When the volume of the plenum is increased sufficiently, a surge condition is encountered. In this case an initial period of rotating stall begins the instability process, and persists as the pressure in the plenum falls through the first part of the surge cycle. The compressor then recovers normal operation, recharging the plenum until the eruption of another rotating stall condition triggers the next surge cycle. The stall cell development process, i.e., the stall cell growth and decay and the process by which the compressor stalls and unstalls, is similar for both the case of pure rotating stall and for the stall condition preceding the surge cycle.

Spatial Domain Analysis

To detail the stall initiation process in its earliest stages, the endwall microphone arrays are utilized in an analysis to detect the rise of pressure waves that exhibit circumferential coherence, indicating a possible precursor to the rotating stall condition.

Rotating Stall

The results from a spatial domain analysis of the first-stage endwall microphones for the case of pure rotating stall are shown in Fig. 4. The top frame presents the rise of the magnitude of the first spatial mode ($n = 1$), with the bottom two frames showing a signal trace from a single wire of a cross-wire probe and the trace from a transducer on the suction side of a first-stage rotor blade. In this figure, the hot-wire and pressure transducer signals have been digitally processed with a 100-Hz low-pass filter. The initial rise in the mode magnitude evident in the top frame corresponds to a sharp disturbance in the hot-wire and pressure transducer signals at $t = 11$ revolutions. From the nonsinusoidal nature of these signal traces the disturbance appears to represent the eruption of a discrete stall cell rather than a growing prestall wave. It should be noted that the mode magnitude trace results from measurements made from the circumferential microphone array in the fixed reference frame, whereas the pressure transducer and hot-wire signals were taken from discrete sensors in the rotating frame. This results in a 1.6 revolution uncertainty in locating the emerging stall cell in the time domain, corresponding to the maximum travel time of the rotating probes to intercept a stall cell propagating at 14 Hz.

The next series of figures presents a more detailed picture of the stall initiation as viewed in the modal domain. In this case, a simultaneous sampling of the microphone signals in all three stages of the compressor was made, with eight microphones utilized in the first stage, and four each in the second and third stages. Figure 5 shows the rise of the magnitude of the first spatial mode and the corresponding phase angular velocity as determined by the eight microphone array upstream of the first rotor row. The phase angular velocity has clearly adjusted to the stall frequency of 14 Hz shortly after the rise of the mode magnitude begins at $t = 38$ revolutions. Early in the signal trace, the phase velocity is poorly defined and appears centered near rotor pass frequency, 37.5 Hz, corresponding to a 1/rev excitation. To verify that this signal corresponds to a pressure wave rather than vibrational excitation of the microphone diaphragm, the experiment was repeated with the microphone static pressure ports sealed. Data from this experiment indicate that vibration and/or electrical noise measurements are at least two orders of magnitude less than the observed pressure magnitudes. It is therefore concluded that the signals shown correspond to an actual pressure disturbance in the compressor. A feature of the phase velocity trace of particular interest is shown at $t = 33$ revolutions, where the wave begins to decelerate to the expected stall frequency. This event begins 5 revolutions prior to the sharp rise in the magnitude of the $n = 1$ mode that was previously shown to accompany the appearance of the stall cell in the rotor blade trace. The mode magnitude over this region exhibits no detectable rise over the background levels.

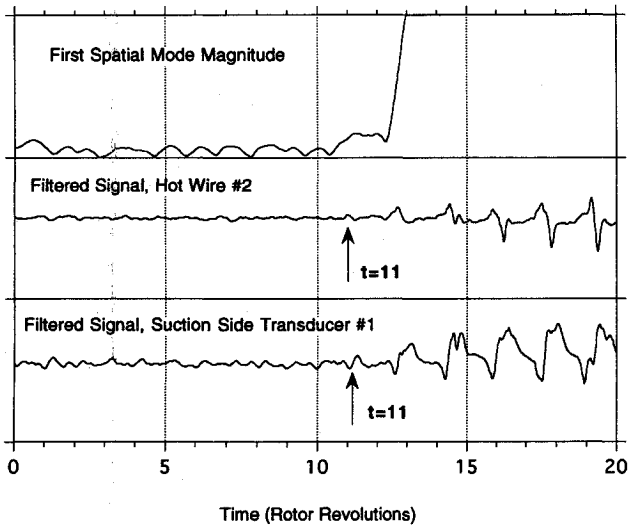

Fig. 4 Rise of the first spatial mode magnitude as compared to the signal from a single hot-wire and rotor-blade pressure transducer for the case of rotating stall.

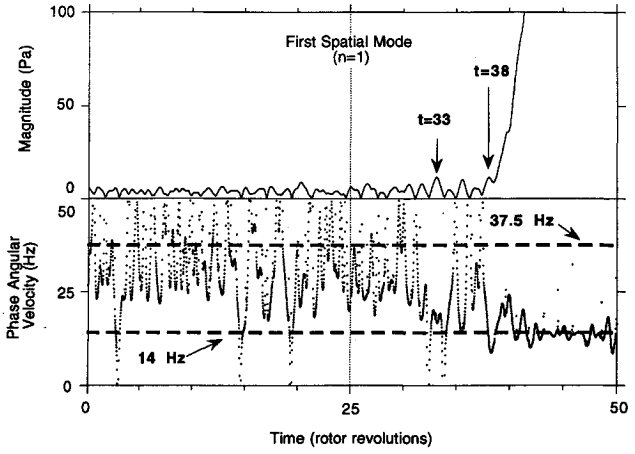

Fig. 5 Rise of the first spatial mode magnitude and phase angular velocity from the first-stage microphone array.

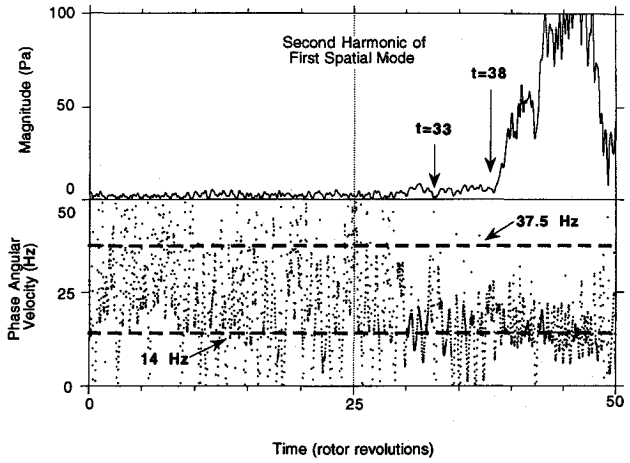

Fig. 6 Rise of the second harmonic of the first spatial mode portrayed in Fig. 5.

As discussed previously, the second harmonic of the $n = 1$ mode will be represented at a frequency twice that of the fundamental and in the $n = 2$ mode. Figure 6 presents the results for the rise of this spatial mode in a frequency band restricted by filtering to a range from 20 to 80 Hz, encompassing the expected 28-Hz second harmonic to the stall condition at 14 Hz. Here, the phase speed shows poor coherence until $t = 31$ revolutions where an adjustment to the eventual phase velocity of the stall pattern ($V_p = 14$ Hz) is shown. At this point a definite, although slight elevation of the mode magnitude is indicated in the top frame of the figure. This adjustment corresponds roughly to the phase adjustment of the first spatial mode shown in the previous figure. Such behavior indicates that the disturbance responsible for the phase velocity change, although small, is distributed nonsinusoidally. This tends to reflect that the microphones are responding to a small flow event near their endwall mounting positions, rather than a global, sinusoidal prestall wave.

A comparison of the rise of the first harmonic magnitude for all three stages is shown in Fig. 7. These data were obtained from the eight microphones in the first stage and the four microphone arrays ahead of the second and third stage rotor rows. This figure demonstrates the simultaneous rise of the first harmonic in all three stages at $t = 25$ revolutions. A detailed view of this point is presented in Fig. 8. As was shown in Fig. 4, this rise coincides with the first signs of a stall cell

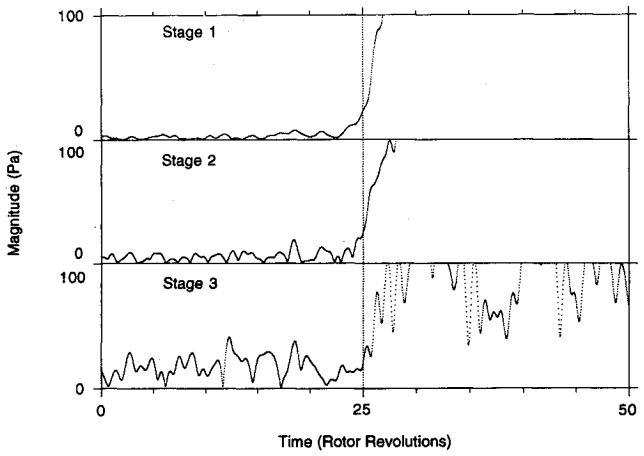

Fig. 7 Comparison of the first spatial mode magnitude at three axial locations.

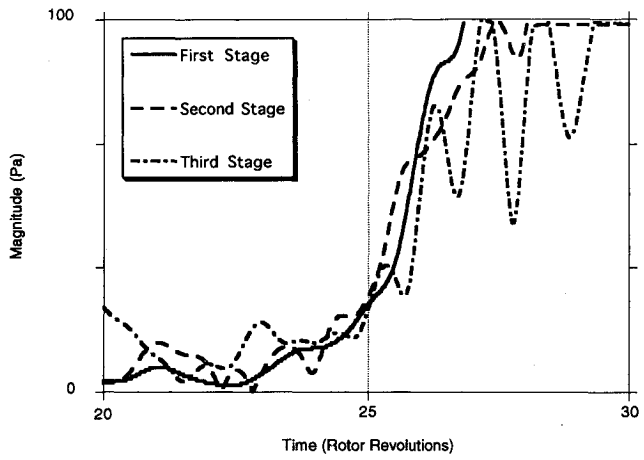

Fig. 8 Detailed view of the rise of the first spatial mode in stages one, two, and three.

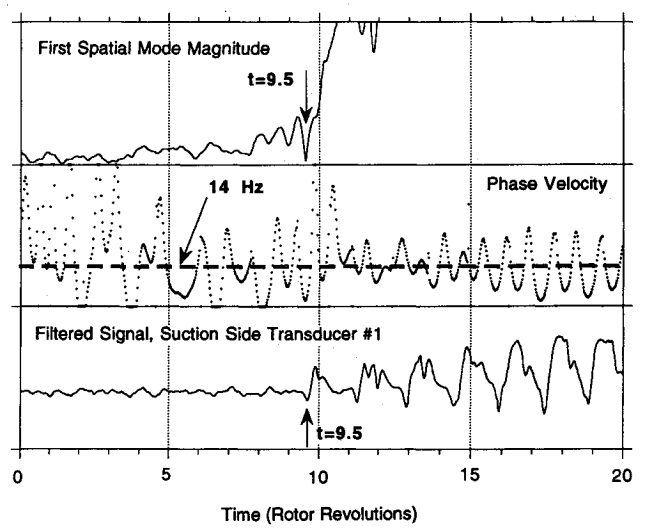

Fig. 9 Rise of the first spatial mode magnitude and phase velocity as compared to the signal from a rotor-blade pressure transducer for the case of rotating stall at the edge of the first surge cycle.

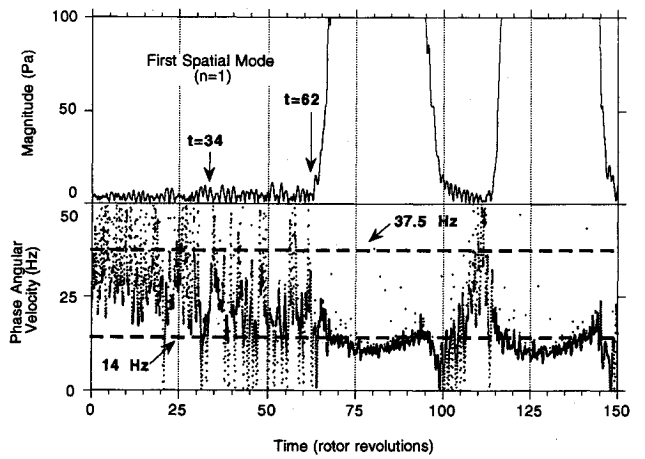

Fig. 10 Rise of the first spatial mode magnitude and phase angular velocity from the first-stage microphone array showing two complete surge cycles.

in the hot-wire and pressure transducer signals. Unfortunately, comparisons between the stages of the mode excitation just prior to this event were inconclusive due to the low signal-to-noise ratio of the signals from the microphones in stages 2 and 3.

Rotating Stall Initiating a Surge Cycle

The compressor exhibits a surge behavior when the plenum volume is increased, with the beginning of each surge cycle marked by a period of rotating stall. Figure 9 shows a comparison as the compressor enters the first surge cycle of the beginning of the rise of the first spatial mode magnitude and the corresponding phase velocity with the signal from the rotor-mounted pressure transducer. As was noted in the previous case, the sharp rise in mode magnitude at $t = 9.5$ revolutions corresponds to the appearance of a stall cell in the blade pressure signal. However, the phase velocity trace indicates that prior to this event, a weak pressure wave has adjusted to the stall frequency of 14 Hz.

A representation of the first mode ($n = 1$) magnitude and phase angular velocity for the first two surge cycles is shown in Fig. 10. These data were taken from the first-stage microphone array. As compared to the earlier case of pure rotating stall, the adjustment of the phase velocity from a rotor speed value to the stall value of 14 Hz can again be seen to precede the sharp rise in mode magnitude at $t = 62$ revolutions. The phase velocity adjustment begins approximately at $t = 34$ revolutions, and continues a gradual deceleration from near rotor pass speed (37.5 Hz) over the next 26 revolutions. The figure shows the recovery from the first surge cycle and subsequent restalling of the compressor, with the phase velocity returning to the 37.5-Hz rotor speed value between these events.

Figure 11 shows the magnitude and phase of the second harmonic of the first spatial mode. The phase velocity trace is quite noisy, but the trend seen in the fundamental $n = 1$ mode is clearly visible. As in the previous case of rotating stall, both the first and second harmonics of the disturbance seem to be excited simultaneously, pointing to an impulsive rather than sinusoidal pressure disturbance.

Details of the rise of the $n = 1$ mode at the beginning of the first surge cycle are presented in Fig. 12. Here, the information from the previous plot is shown on a smaller time scale to clearly show the adjustment of a weak disturbance from the 37.5-Hz phase velocity to the eventual 14-Hz value for the developed stall cell. Little change in the mode magnitude is found to accompany this event, with quite oscillatory behavior evident. This behavior is reflected in the noisy character of the phase velocity trace. The second harmonic of this mode is shown in Fig. 13. Here, the mode magnitude begins to rise from the background level as early as $t = 34$ revolutions, with corresponding adjustment of the phase velocity to the expected stall frequency of 14 Hz. It is considered likely that the improved resolution in the rise of the second harmonic magnitude is due to the low magnitude of any rotor-

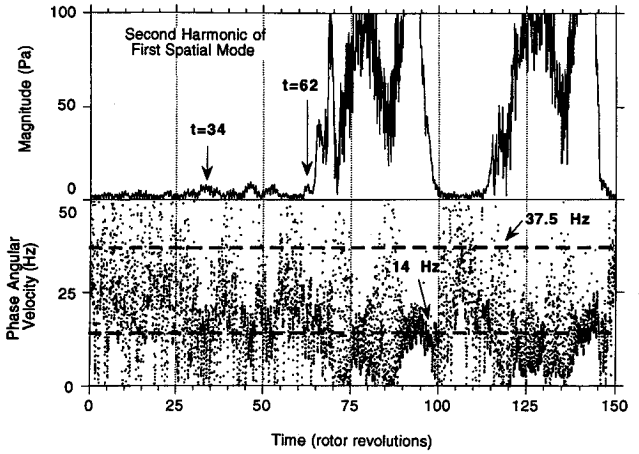

Fig. 11 Rise of the second harmonic of the first spatial mode portrayed in Fig. 10.

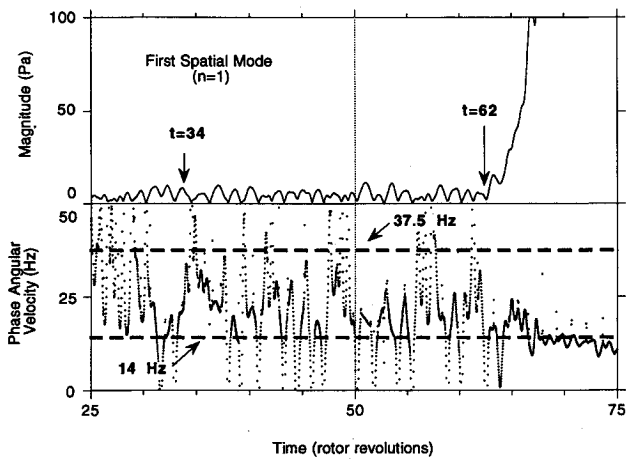

Fig. 12 Detailed view of rotating stall initiation at the edge of the first surge cycle. Magnitude of the first spatial mode and the phase angular velocity are shown.

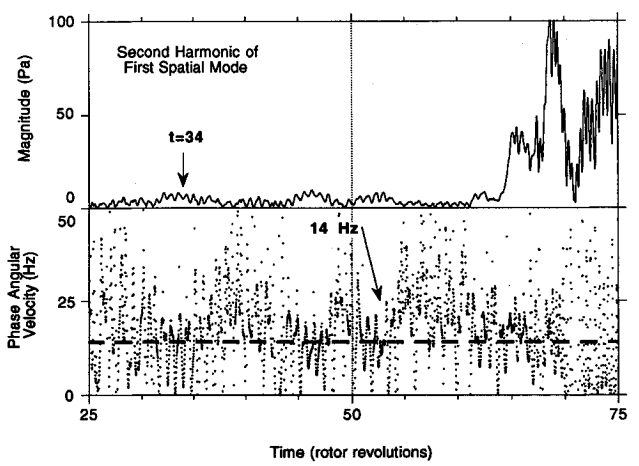

Fig. 13 Rise of the second harmonic of the first spatial mode portrayed in Fig. 12.

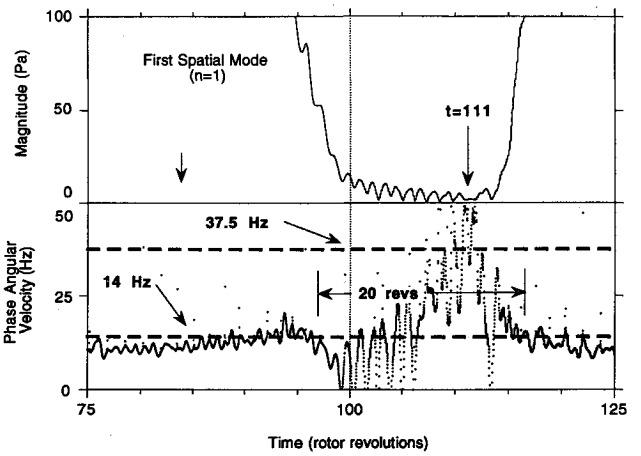

Fig. 14 Detailed view of rotating stall recovery and restalling at the start of second surge cycle. Magnitude of the first spatial mode and the phase angular velocity are shown.

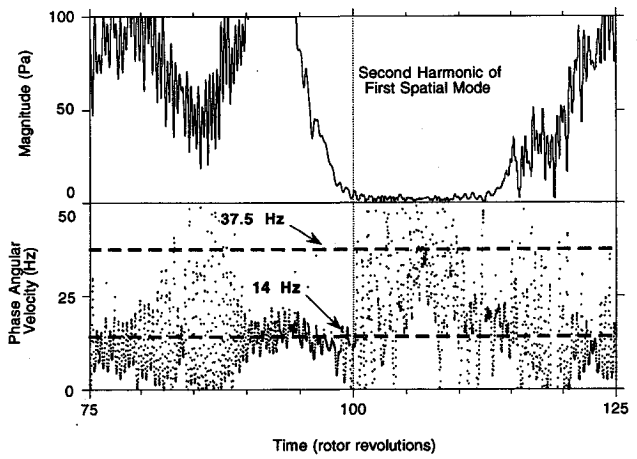

Fig. 15 Rise of the second harmonic of the first spatial mode portrayed in Fig. 14.

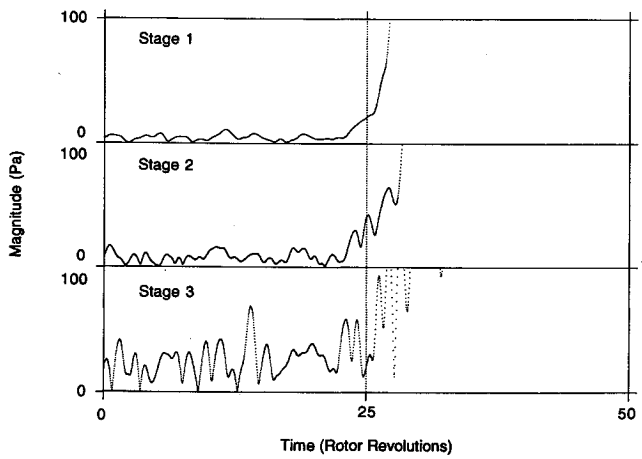

Fig. 16 Comparison of the first spatial mode magnitude at three axial locations for the start of the first surge cycle.

speed order disturbance when compared to the fundamental $n = 1$ mode.

A similar picture for the recovery and restalling of the compressor as it enters the second surge cycle is shown in Fig. 14. Here, the fundamental mode magnitude falls to the prestall level, with an accompanying rise in the first mode phase velocity to the rotor-speed value of 37.5 Hz. The phase velocity begins to decrease as soon as that value is reached, falling as the compressor restalls. The second harmonic is shown in Fig. 15, with the results close to those seen in the fundamental harmonic. The adjustment of the phase velocity to the eventual stalling frequency occurs within 5 revolutions for the second surge cycle as compared to the 26 revolutions seen for the first surge cycle.

The picture of the stalling process derived from the above figures again seems to indicate an impulsive-type waveform

in the spatial domain, as was deduced for the case of pure rotating stall. This would indicate a small, propagating separated flow region in the region near the first rotor row.

A view of the rise of the $n = 1$ mode magnitude in each of the three stages is shown in Fig. 16. As in the previous case, all three stages show the rise of the magnitude occurring simultaneously.

Summary and Conclusions

The objective of this investigation was to identify spatially coherent pressure waves that would serve as precursors to the development of an instability in the PAFRC. To achieve this, sensitive electret microphones were uniformly distributed around the circumference of the compressor. Fourier analysis of simultaneously sampled data from these microphone arrays was utilized to identify the development of dominant spatial modes in the pressure field in the compressor. The transition to stall was observed to be an abrupt process, with the eruption of a stall cell on rotor blades corresponding to a strong rise in the spatial mode magnitude. However, a weak, circumferentially distorted pressure wave was detected that began adjusting to the ultimate phase propagation velocity of the finite stall pattern from within 5 to 26 revolutions prior to a significant rise in the mode magnitude and the indication of a stall cell from the rotor blade pressure transducers. Comparison of the first and second harmonics of this signal indicate that this disturbance is represented in the spatial domain by an impulsive-type waveform. Because the microphones were mounted near the rotor blades (0.3 chords upstream), they were ideally placed to accurately characterize separation events near the rotor o.d. endwall without decay of the higher harmonics that would be encountered with sensors mounted further upstream in the inlet.

The early excitation of the spatial modes was more easily detected in traces of the second mode ($n = 2$) rather than the $n = 1$ mode that characterized the stalling behavior. Nevertheless, this mode is classified as a second harmonic of the first mode rather than an independent $n = 2$ mode based on the observed phase propagation velocity. The ease in detecting the $n = 2$ mode can be attributed to the presence of a weak rotor-speed disturbance in the first mode ($n = 1$), which was clearly stronger than any 2/rev rotor speed excitation. This resulted in an improved signal-to-noise ratio for signals in the second mode.

The impulsive nature of the weak pressure disturbance prior to stall suggests that these events represent a short length scale event in the compressor that is propagating around the annulus. However, this does not necessarily prevent the classification of these disturbances as prestall waves, as small separation zones clearly would result in a distortion of the potential core flow of the compressor, and such a potential distortion would in turn result in conditions favorable for the formation of propagating separation zones. The question that is of greatest importance is not the causal relationship between short- and long-scale phenomena in the compressor, but rather which type of disturbance is more economically usable in a stall avoidance/control scheme. The answer to this question lies in further experimentation with stall control systems employing a variety of control mechanisms.

Acknowledgment

Support of this research by the U.S. Army Research Office is most gratefully acknowledged.

References

[1]Pinsley, J. E., Guenette, G. R., Epstein, A. H., and Greitzer, E. M., "Active Stabilization of Centrifugal Compressor Surge," *Journal of Turbomachinery*, Vol. 113, Oct. 1991, pp. 723–732.

[2]Ffowcs Williams, J. E., and Graham, W. R., "An Engine Demonstration of Active Surge Control," American Society of Mechanical Engineers Paper 90-GT-224, June 1990.

[3]Day, I. J., "Active Suppression of Rotating Stall and Surge in Axial Compressors," *Journal of Turbomachinery*, Vol. 115, Jan. 1993, pp. 40–47.

[4]Paduano, J., Epstein, A. H., Valavani, L., Longley, J. P., Greitzer, E. M., and Guenette, G. R., "Active Control of Rotating Stall in a Low Speed Axial Compressor," *Journal of Turbomachinery*, Vol. 115, Jan. 1993, pp. 48–56.

[5]Garnier, V. H., Epstein, A. H., and Greitzer, E. M., "Rotating Waves as a Stall Inception Indication in Axial Compressors," *Journal of Turbomachinery*, Vol. 113, April 1991, pp. 299–302.

[6]Emmons, H. W., Pearson, C. E., and Grant, H. P., "Compressor Surge and Stall Propagation," *Transactions of the American Society of Mechanical Engineers*, Vol. 79, April 1955, pp. 455–469.

[7]Day, I. J., "Stall Inception in Axial Flow Compressors," *Journal of Turbomachinery*, Vol. 115, Jan. 1993, pp. 1–9.

[8]McDougall, N. M., Cumpsty, N. A., and Hynes, T. P., "Stall Inception in Axial Compressors," *Journal of Turbomachinery*, Vol. 112, Jan. 1990, pp. 116–125.

[9]Lawless, P. B., and Fleeter, S., "Rotating Stall Acoustic Signature in a Low Speed Centrifugal Compressor, Part 1: Vaneless Diffuser," American Society of Mechanical Engineers Paper 93-GT-297, May 1993.

[10]Kim, K., and Fleeter, S., "Compressor Unsteady Aerodynamic Response to Rotating Stall and Surge Excitations," AIAA Paper 93-2087, June 1993.